Precipitation Kinetics and Morphology of Grain Boundary Carbides in Ni-Base Superalloy Haynes 282

Communication

Precipitation Kinetics and Morphology of Grain Boundary Carbides in Ni-Base Superalloy Haynes 282

C. JOSEPH, C. PERSSON, and
M. HÖRNQVIST COLLIANDER

Precipitation of grain boundary carbides in a mill-annealed Haynes 282 in the temperature range 650 °C to 1120 °C was investigated. The kinetics of $M_{23}C_6$ was significantly faster than that of M_6C. With increasing aging temperature, the morphology changes from continuous film to an interconnected brick wall structure and finally to discrete particles. No morphological changes were observed with aging time. Serrated grain boundaries formed during aging around 750 °C. The solvus temperature for both $M_{23}C_6$ and M_6C was approximately 1100 °C.

https://doi.org/10.1007/s11661-020-06019-1

The newly developed Ni-based superalloy Haynes 282 is specifically aimed for high-temperature applications in components for aero- and land-based turbine engines because of its excellent high-temperature creep resistance and strength, fabricability and superior weldability.[1–4] As in other superalloys, the mechanical properties are primarily governed by the morphology and distribution of precipitated phases in the microstructure, where gamma prime (γ') imparts strength while the carbides at the grain boundaries contribute to the good creep resistance. The conventional heat treatment of Haynes 282 is a two-step aging at 1010 °C/2 hours/AC and 788 °C/8 hours/AC, where AC denotes air cooling, which is carried out directly on mill-annealed material. The first aging step stabilizes the desired grain boundary carbides, and the second aging step precipitates γ'. A recent study showed that the morphology of grain boundary carbides can significantly affect the tensile ductility of Haynes 282.[5] When carbides were present in an interconnected "brick wall" structure, the ductility decreased by almost 50 pct compared to material with discrete carbides in the grain boundaries. Fahrmann and Pike[6] studied the kinetics of secondary carbide formation in Haynes 282 and showed that the precipitation of M_6C was significantly slower than expected. Polkowska *et al.*[7] showed that the temperature stability of M_6C was higher than that of $M_{23}C_6$, as the latter did not appear after aging at ≥ 1010 °C. This is contradictory to the results presented in Reference 6, where both $M_{23}C_6$ and M_6C were observed up to 1100 °C.

However, a systematic study of the grain boundary carbide morphology has not yet been reported, which appears to be warranted given the previously observed effect on tensile ductility[5] and known reduction in creep resistance for superalloys.[8–10] It is also important for the development of alternative heat treatments, such as the single-stage aging proposed in Reference 11, where the stabilization treatment was omitted and carbides were instead precipitated together with γ' at 800 °C. The objective of this work is therefore to characterize the carbide morphology development in Haynes 282 with temperature and time, as there are insufficient literature data on the phase stability and precipitation in this newly developed alloy. To this end, we subjected a mill-annealed Haynes 282 sheet to aging heat treatments in the temperature range 650 °C to 1120 °C and examined the precipitated phases using scanning electron microscopy (SEM) and energy-dispersive X-ray spectroscopy (EDS) analysis.

The samples were taken from a 3-mm-thick Haynes 282 sheet, manufactured as per specification AMS5951. The chemical composition according to the supplier material certificate is given in Table I. The typical mill-annealing treatment consists of a solution treatment in the temperature range 1121–1177 °C for an unknown time followed by air cooling. No further information regarding the processing history was available for the material in the present study. Samples of 10 × 10 × 3 mm^3 size were cut from the sheets and heat treated in air using a box furnace. In the temperature range from 650 °C to 980 °C heat treatments were carried out for times ranging from 2 minutes to 98 hours, whereas at higher temperatures (between 1000 °C and 1120 °C) times from 2 minutes to 2 hours were used. The samples were water quenched after heat treatment.

For microstructural studies, the samples were ground and polished using an alumina suspension. They were ultrasonically cleaned and subsequently electrolytically etched with oxalic acid etchant to allow grain boundary carbides to be studied using SEM and (on selected specimens at specific temperatures) EDS for semiquantitative information on the carbides at the grain

C. JOSEPH is with the Department of Industrial and Materials Sciences, Chalmers University of Technology, 41296, Göteborg, Sweden and also with the GKN Aerospace Engine Systems AB, 461 38, Trollhättan, Sweden. C. PERSSON is with the Department of Industrial and Materials Sciences, Chalmers University of Technology. M. HÖRNQVIST COLLIANDER is with the Department of Physics, Chalmers University of Technology, 41296 Göteborg, Sweden. Contact e-mail: magnus.colliander@chalmers.se

Manuscript submitted July 3, 2020 and accepted September 4,2020.

Published online: 06 October 2020

boundaries. Samples for hardness testing were prepared and tested according to ASTM standard E92. The Vickers macro-hardness of samples was measured with a 10-kg load, and an average of five measurements is reported in this study.

The microstructure of the mill-annealed sheet consists of equiaxed grains of the order of ~100 μm with MC carbides (rich in Ti and Mo) and carbonitrides distributed in the rolling direction both inter- and intragranularly (see[5] for details). No γ' particles could be observed by SEM, and the grain boundaries were mainly free from carbides, although occasional isolated grain boundary carbides could be found. The hardness of the mill-annealed material was measured to be 241 HV, higher than for the same material in the solution-treated and water-quenched state,[5] which indicates the presence of γ' with size below the SEM resolution limit as reported for the mill-annealed state in Reference 6.

Figure 1 shows micrographs of samples aged for 2 hours at different temperatures. With increasing temperature, the carbide morphology changes from a film-like appearance at lower temperatures (< 750 °C) to a brick morphology and finally a discrete morphology at higher aging temperatures (> around 850 °C). Carbide film formation at low temperatures (732 °C to 760 °C) has previously been reported in a Ni-based superalloy,[8]

Table I. Chemical Composition of Haynes 282 Sheet Material (Wt Pct)

Ni	Cr	Co	Mo	Ti	Al	Fe	C	B	P	S	Si
Bal.	19.63	10.35	8.56	2.21	1.41	0.35	0.068	0.004	0.002	0.002	0.05

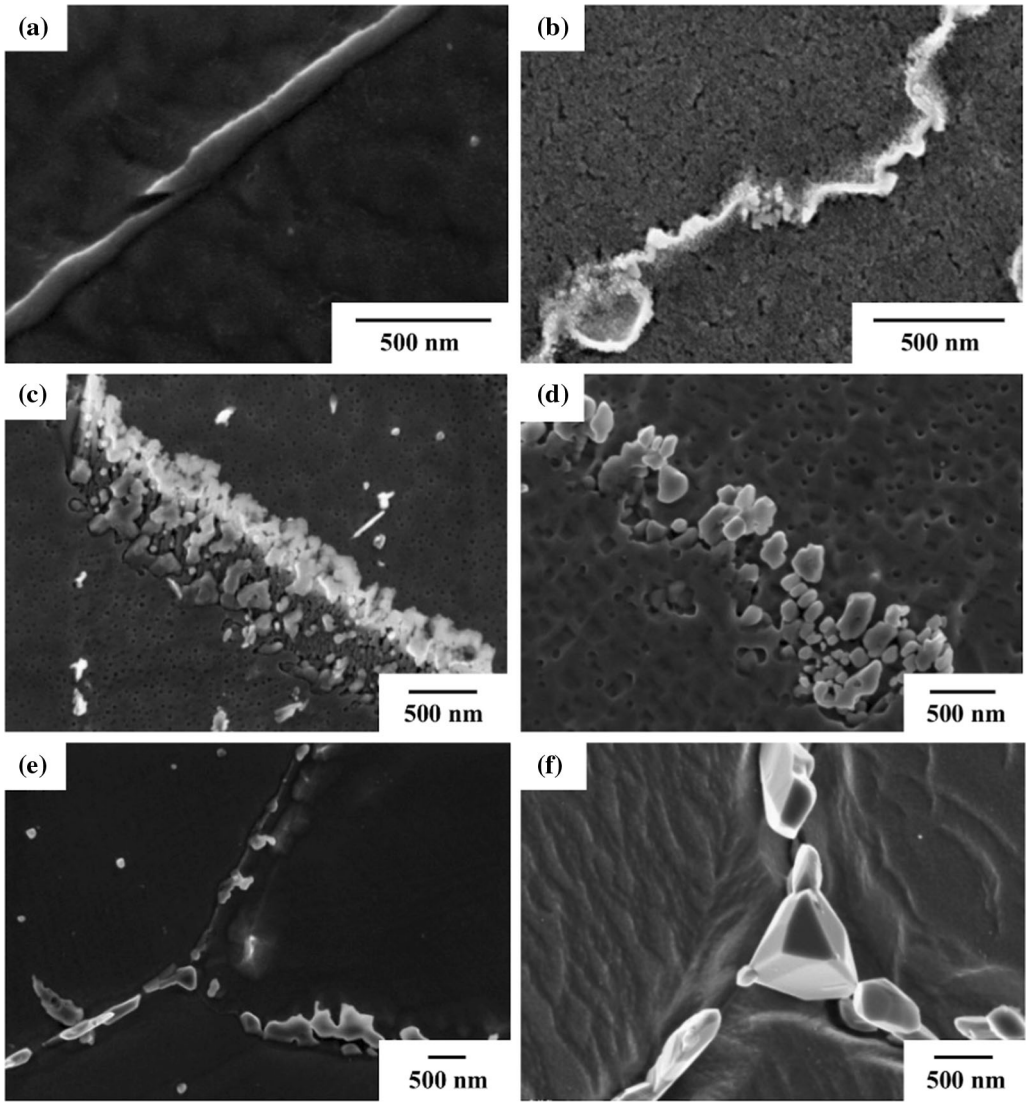

Fig. 1—SEM images showing the morphology of the grain boundary carbides after 2 h aging at different temperatures: (*a*) 650 °C, (*b*) 750 °C, (*c*) 850 °C, (*d*) 950 °C, (*e*) 1000 °C, (*f*) 1050 °C.

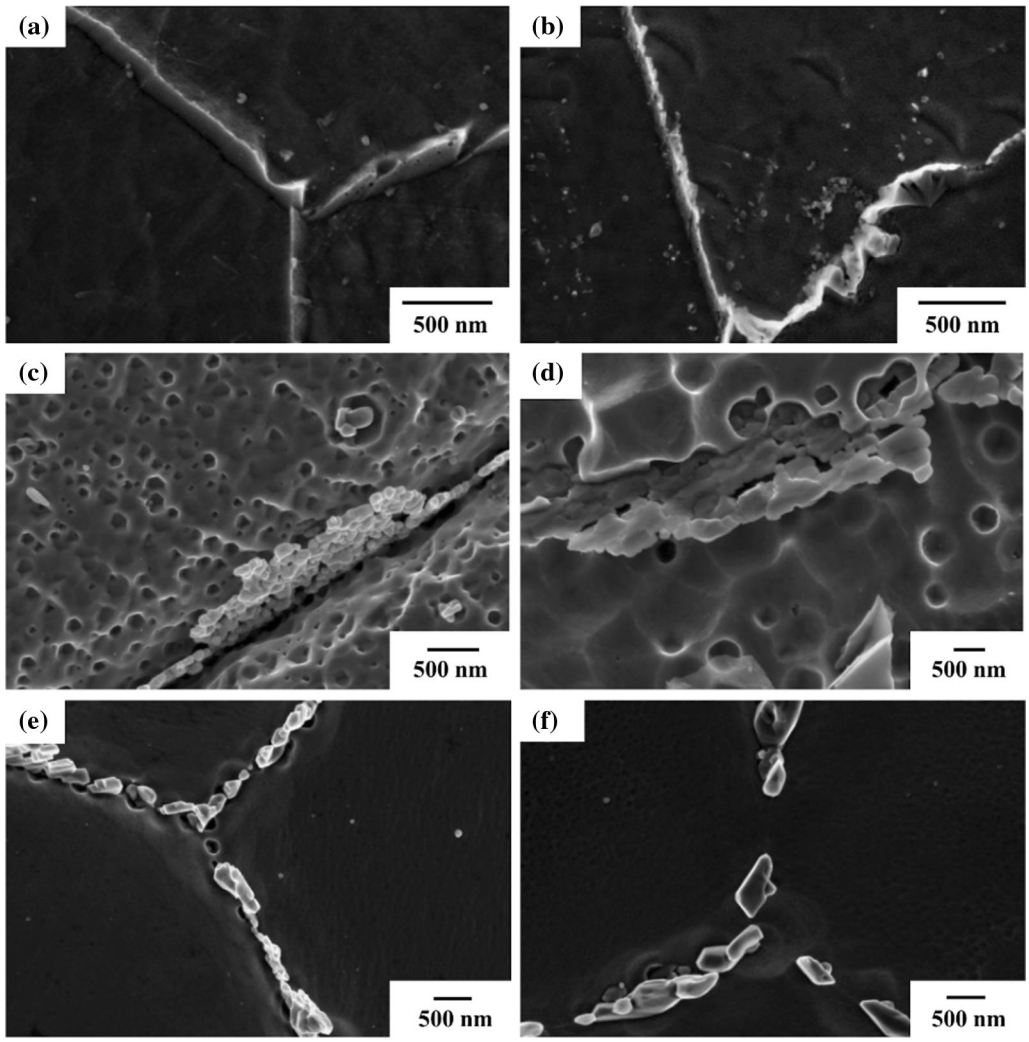

Fig. 2—SEM images show that there are no morphological changes in the grain boundary carbides with aging time at 650 °C (film morphology) for (*a*) 30 min, (*b*) 50 h; 950 °C (brick morphology) for (*c*) 2 h, (*d*) 26 h; and 1000 °C (discrete morphology) for (*e*) 2 h and (*f*) 26 h.

and this specific morphology is particularly detrimental for the stress-rupture resistance of material.[8,10] We also note the serrated gain boundaries observed after 2 hours aging at 750 °C (Figure 1(b)). Such serrated grain boundaries have been previously reported in Haynes 282 after slow cooling (0.05 °C s^{-1}) from 1135 °C.[12] Formation of serrated boundaries during slow cooling and a resulting beneficial effect on the creep behavior have been reported for several Ni-base superalloys.[13–16] The present results shows that grain boundary serrations can also form during low-temperature annealing. At much higher aging temperatures, > 1100 °C, the carbides completely dissolve and the grain boundaries are free from carbides. At a particular aging temperature there is no major change in grain boundary carbide morphology with time, as shown in Fig. 2, but rather a gradual growth and coarsening.

Figure 3 shows an example of an EDS map of grain boundaries with carbides, obtained after aging at 800 °C for 98 hours. $M_{23}C_6$ (Cr-rich) and M_6C (Mo-rich) can be easily separated based on chemical information from EDS (see Table II), which allowed identification of their respective presences. It should be noted that EDS analyses were only performed on selected specimens at specific combinations of aging temperatures and aging times. For the remaining specimens, only the presence or absence of carbides was recorded, as it was in many cases difficult to separate the different types based on morphology.

A summary of the experimental observations for the carbides, including the TTT curves proposed by Fahrmann and Pike,[6] is presented in Figure 4. Note that the locations of the TTT curves are only approximate and do not correlate to a specific volume fraction of carbides. The two studies are largely consistent, and our results confirm the slow kinetics of M_6C precipitation and the similar solvus temperatures of $M_{23}C_6$ and M_6C around 1100 °C. The discrepancy between these observations and the results obtained by Polkowska *et al.*[7] could arise from the different starting conditions used. Here, and in Reference 6, mill-annealed sheet was used, whereas Polkowska *et al.*[7] indicated an initial

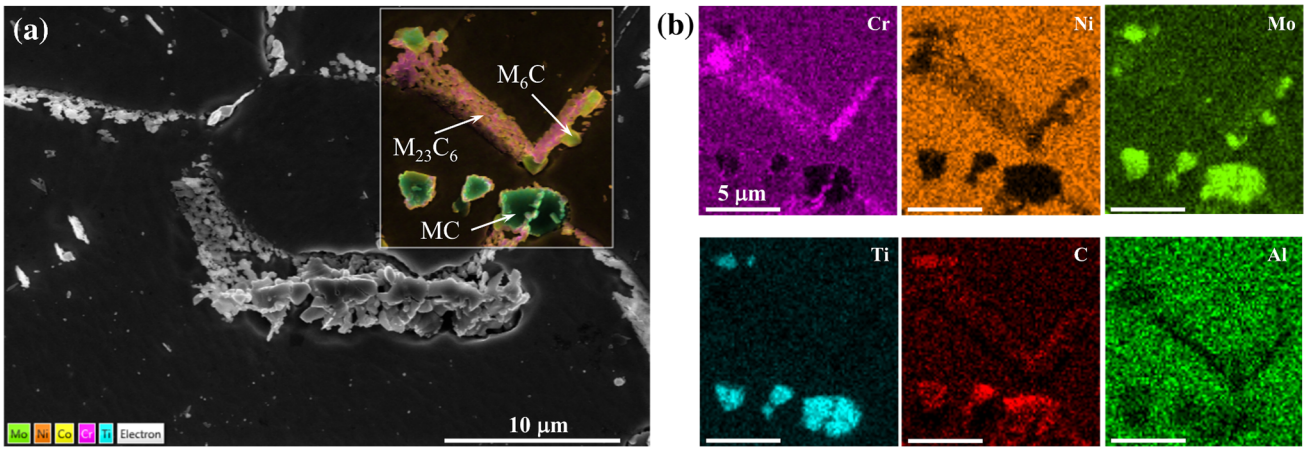

Fig. 3—Analysis of grain boundary carbides obtained after aging at 800 °C for 98 h. (*a*) SEM image, indicating the different carbides. (*b*) EDS maps of the region shown in (a).

Table II. Chemical Composition of Carbides Detected by EDS Analysis (Wt Pct)

Carbide	Ni	Mo	Cr	C	Co	Ti	Al
M_6C	20.16	48.55	14.57	5.84	7.86	2.36	0.35
$M_{23}C_6$	4.82	22.91	65.86	6.41	—	—	—

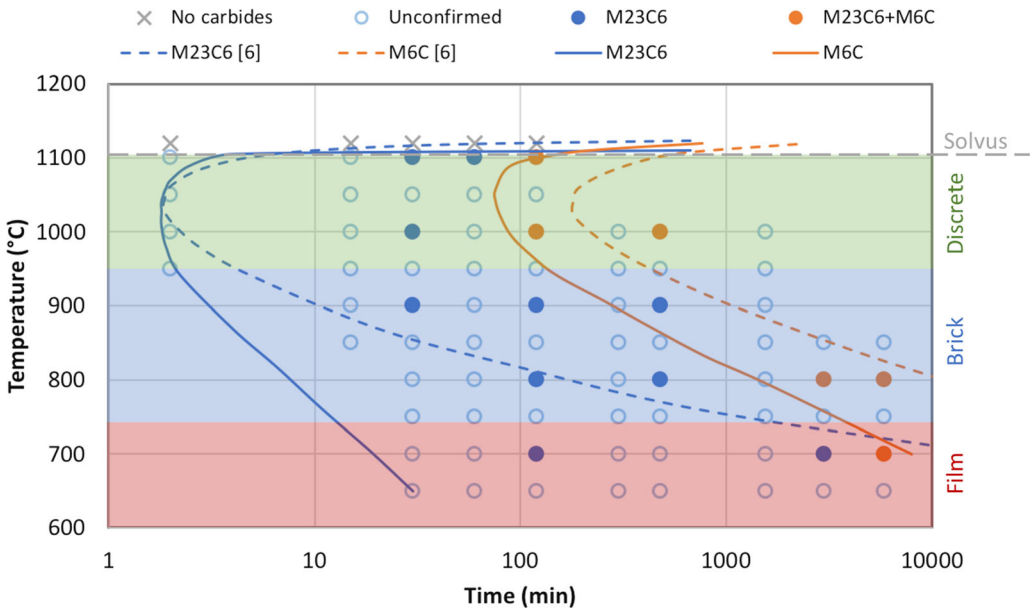

Fig. 4—Experimentally determined TTT diagram compared to the previously reported curves by Fahrmann and Pike.[6] "Unconfirmed" in the legend refers to observed carbides that were not further identified.

solution treatment at 1150 °C in their graphical representation of the heat treatment (although not further described in the text). As solution treatment > around 1120 °C will lead to rapid grain growth,[17] the movement of grain boundaries away from their initial position, around which C can be expected to be enriched, could alter the local chemistry and therefore carbide precipitation behavior. Related observations were made in Reference 5, where grain growth during solution treatment actually suppressed the formation of carbides during the 1010 °C stabilization treatment, which led to carbide precipitation in the detrimental

interconnected ''brick wall'' network at the second aging temperature (788 °C) and the resulting loss of ductility. Notably, the formation of a ''brick wall'' morphology at 788 °C when carbide precipitation at 1010 °C was suppressed[5] is consistent with the present observations.

There are, however, some noticeable differences between our observations and the TTT curves proposed in Reference 6. Carbides are present after shorter aging times in the present study, and even at the lowest aging temperature (650 °C) carbides are seen already after 30 minutes. This can be explained by the absence of shorter aging times in Reference 6 and because the proposed TTT curve for $M_{23}C_6$ in Reference 6 was based on confirmed $M_{23}C_6$ observations only, although unconfirmed carbides were observed at shorter times. Here we assume that also unconfirmed carbides observed at short times are $M_{23}C_6$, since M_6C does not precipitate much later. The faster M_6C kinetics observed here can, at least in part, be explained by the smaller time steps, which allow a more precise identification of the onset of precipitation. Consequently, there are no contradictions between our results and the observations in Reference 6. Notably, the sluggish M_6C precipitation suggests that $M_{23}C_6$ should dominate after most, if not all, commercial heat treatments. Nevertheless, Polkowska *et al.*[7] reported the presence of M_6C at all temperatures after 2 hours aging at 900 and 1050 °C. Contrarily, in the present study no M_6C could be found even after 8 hours at 900 °C. The exact same temperature was not investigated in Reference 6, but no M_6C was reported after 10 hours at 871 °C. The agreement between this study and[6] and the different behavior observed in Reference 7 appear to suggest that not only stability, but also kinetics could be sensitive to prior solution treatments.

Finally, we note that no other phases (such as σ or μ) were observed, consistent with the reports after long-term thermal exposure.[18] The Mo-rich grain boundary borides previously reported by Osoba *et al.*[19] were not observed. This is consistent with,[6] where the suggested reason for the absence of borides was either the very small size and volume fraction or the possible formation of $M_{23}(C,B)_6$ rather than separate borides.

In summary, we confirm the observation by Fahrmann and Pike[6] regarding precipitation of $M_{23}C_6$ and M_6C at the grain boundaries in Haynes 282, and in particular the slow kinetics of M_6C. We furthermore report a temperature (but not time) dependence of the morphology of the secondary carbides. With increasing aging temperature, the morphology changes from the continuous film to brick wall structure and finally to discrete particles, which can have significant implications for the ductility and creep resistance of the material. No further morphological changes were observed with increasing aging time; only a growth and coarsening of the carbides occurred. Serrated grain boundaries, which are otherwise usually observed after slow cooling, developed during aging at 750 °C. We also note that both $M_{23}C_6$ and M_6C exist up to 1100 °C.

The funding for the present work has been provided by the Swedish Agency for Innovation (VINNOVA), through the Swedish National Aeronautical Research Program (NFFP) Grant Nos. 2010-01221 and 2013-01154, which are gratefully acknowledged. GKN Aerospace Engine Systems AB is kindly acknowledged for supplying the material.

Open access funding provided by Chalmers University of Technology.

REFERENCES

1. L.M. Pike, Development of a Fabricable Gamma-Prime (γ') Strengthened Superalloy (Paper presented at Superalloys 2008, Champion, PA, September 14-18, 2008), pp 191-200.
2. L. M. Pike, Haynes 282 Alloy - A New Wrought Superalloy Designed for Improved Creep Strength and Fabricability (Paper presented at ASME Turbo Expo 2006).
3. K.L. Kruger: in *Materials for Ultra-Supercritical and Advanced Ultra-Supercritical Power Plants*. A. Di Gianfrancesco, Woodhead Publishing, 2017, pp. 511–45.
4. S.K. Srivastava, J.L. Caron, and L.M. Pike: *Advances in Materials Technology for Fossil Power Plants - Proceedings from the 7th International Conference*, HI, Waikoloa, 2014, pp. 120–30.
5. C Joseph, C Persson, and MH Colliander: *Mater. Sci. Eng. A*, 2017, vol. 697, pp. 520–30.
6. M. G. Fahrmann, L.M. Pike: *Proc. 9th Int. Conf. on Superalloy 718 and Derivatives*, TMS, 2018, Pittsburgh, PA, pp. 566–78.
7. A. Polkowska, W. Polkowski, M. Warmuzek, N. Ciesta, G. Wloch, D. Zasada, and R.M. Purgent: *J. Mater. Eng. Perform.*, 2019, vol. 28, pp. 3844–51.
8. T.J. Garosshen and G.P. McCarthy: *Metall. Trans.*, 1985, vol. 16A, pp. 1213–23.

9. M.C. Pandey, D.V.V. Satyanarayana, and D.M.R. Taplin: *Mater. Sci. Technol.*, 1994, vol. 10, pp. 936–39.
10. D.L. Shu, S.G. Tian, N. Tian, J. Xie, and Y. Su: *Mater. Sci. Eng. A*, 2017, vol. 700, pp. 152–61.
11. J. R. Robertson: *Proceedings of the ASME 2018 Symposium on Elevated Temperature Application of Materials for Fossil, Nuclear, and Petrochemical Industries - ETAM2018*, 2018, Seattle, WA, V001T01A007.
12. K.-Y. Shin, J.-H. Kim, M. Terner, B.-O. Kong, and H.-U. Hong: *Mater. Sci. Eng. A*, 2019, vol. 751, pp. 311–22.
13. A. Wisniewski and J. Beddoes: *Mater. Sci. Eng. A*, 2009, vols. 510–511, pp. 266–72.
14. A.-C. Yeh, K.-W. Lu, C.-M. Kuo, H.-Y. Bor, and C.-N. Wei: *Mater. Sci. Eng. A*, 2011, vol. 530, pp. 525–29.
15. J.G. Yoon, H.W. Jeong, Y.S. Yoo, and H.U. Hong: *Mater. Char.*, 2015, vol. 101, pp. 49–57.
16. Y.T. Tang, A.J. Wilkinson, and R.C. Reed: *Metall. Mater. Trans.*, 2018, vol. 49A, pp. 4324–42.
17. S. Suhas: *Effect of solutionizing heat treatment on microstructure and properties of nickel based superalloy Haynes 282*, M.Sc. Thesis, Chalmers University of Technology, 2016.
18. L.M. Pike: *Proc. 7th Int. Conf. on Superalloy 718 and Derivatives*, TMS, 2010, Pittsburgh, PA, pp. 645–60.
19. L.O. Osoba, R.G. Ding, and O.A. Ojo: *Metall. Mater. Trans.*, 2012, vol. 43A, pp. 4281–95.